

# Capture rate and neutron helicity asymmetry for ordinary muon capture on hydrogen

Shung-ichi Ando,\* Fred Myhrer,<sup>†</sup> and Kuniharu Kubodera<sup>‡</sup>

*Department of Physics and Astronomy, University of South Carolina, Columbia, South Carolina 29208*

(Received 9 August 2000; published 20 December 2000)

Applying heavy-baryon chiral perturbation theory to ordinary muon capture (OMC) on a proton, we calculate the capture rate and neutron helicity asymmetry up to next-to-next-to-leading order. For the singlet hyperfine state, we obtain the capture rate  $\Gamma_0=695\text{ s}^{-1}$  while, for the triplet hyperfine state, we obtain the capture rate  $\Gamma_1=11.9\text{ s}^{-1}$  and the neutron asymmetry  $\alpha_1=0.93$ . If the existing formalism is used to relate these atomic capture rates to  $\Gamma_{\text{liq}}$ , the OMC rate in liquid hydrogen, then  $\Gamma_{\text{liq}}$  corresponding to our improved values of  $\Gamma_0$  and  $\Gamma_1$  is found to be significantly larger than the experimental value, primarily due to the updated larger value of  $g_A$ . We argue that this apparent difficulty may be correlated to the specious anomaly recently reported for  $\mu^-+p\rightarrow n+\nu_\mu+\gamma$ , and we suggest a possibility to remove these two ‘‘problems’’ simply and simultaneously by reexamining the molecular physics input that underlies the conventional analysis of  $\Gamma_{\text{liq}}$ .

DOI: 10.1103/PhysRevC.63.015203

PACS number(s): 24.85.+p, 11.80.Cr, 12.39.Fe, 23.40.-s

## I. INTRODUCTION

Muon capture on a proton is a valuable source of information about  $g_P$ , the pseudoscalar coupling constant of the nucleon weak current [1]. One can study two processes, ordinary muon capture (OMC) and radiative muon capture (RMC)<sup>1</sup>:

$$\mu^-+p\rightarrow\nu_\mu+n\quad(\text{OMC}),\quad(1)$$

$$\mu^-+p\rightarrow\nu_\mu+n+\gamma\quad(\text{RMC}).\quad(2)$$

Heavy-baryon chiral perturbation theory (HBChPT) is well suited for describing these processes, which involve small enough energy-momentum transfers to render the HBChPT series rapidly convergent. We report here our HBChPT calculation for OMC up to next-to-next-to-leading order. To explain the motivation and significance of our work, we first describe briefly the current status of OMC and RMC.

The OMC rate in liquid hydrogen,  $\Gamma_{\text{liq}}$ , has been measured with 5% accuracy [2]:

$$\Gamma_{\text{liq}}^{\text{exp}}=460\pm 20\quad[\text{s}^{-1}].\quad(3)$$

Theoretically, one first calculates the atomic OMC rates for a proton,  $\Gamma_0$  and  $\Gamma_1$ , where the suffix ‘‘0’’ (‘‘1’’) refers to the singlet (triplet) hyperfine state of the hydrogen atom. To compare with experiment, one needs a theoretical framework to relate  $\Gamma_0$  and  $\Gamma_1$  to  $\Gamma_{\text{liq}}$ . For convenience, we refer to this framework as the ‘‘atom-liquid’’ translation formulas. A great deal of experimental and theoretical effort has been invested on these translation formulas [3]. In Refs. [1,4],  $\Gamma_0$  and  $\Gamma_1$  were calculated using the phenomenologically parametrized weak nucleon form factors with the value of  $g_P$  obtained from the partially conserved axial current (PCAC).

If we combine these estimates with the existing atom-liquid translation formulas, the resulting  $\Gamma_{\text{liq}}^{\text{th}}$  agrees with  $\Gamma_{\text{liq}}^{\text{exp}}$  within the experimental error [3]. In HBChPT,  $\Gamma_0$  and  $\Gamma_1$  were calculated up to next-to-leading order (NLO) by Bernard *et al.* [5]; it was also reported that a one-loop level calculation reproduces the known analytical PCAC correction for  $g_P$ , see Refs. [6,7]. On the other hand, the precise empirical determination of  $g_P$  is hampered by the 5% error in  $\Gamma_{\text{liq}}^{\text{exp}}$ ; the sensitivity of  $\Gamma_{\text{liq}}^{\text{exp}}$  to  $g_P$  is rather modest because the fixed momentum transfer in OMC ( $q^2=-0.88m_\mu^2$ ) suppresses the contribution of the  $g_P$  term, which contains the pion-pole structure  $\sim 1/(q^2-m_\pi^2)$ .

Since RMC is free from this kinematic constraint, it can be a more sensitive probe of  $g_P$ , despite its extremely small branching ratio. A recent TRIUMF experiment succeeded in measuring  $d\Gamma_{\text{RMC}}/dE_\gamma$ , the absolute photon spectrum for RMC in liquid hydrogen [8,9]. If one uses atomic RMC amplitudes calculated in the phenomenological minimal coupling method [10], and if one adopts the existing atom-liquid translation formulas, then the observed  $d\Gamma_{\text{RMC}}/dE_\gamma$  cannot be reproduced unless  $g_P$  is artificially increased from its PCAC value by as much as 50%. However, such a large deviation of  $g_P$  from its PCAC value is extremely unlikely according to an HBChPT calculation [6]. This very astonishing feature reported for  $d\Gamma_{\text{RMC}}/dE_\gamma$  motivated reexamination of the formalism used in Ref. [10] to calculate the RMC amplitude, and several calculations based on HBChPT have been carried out [5,11,12]. A next-to-leading order (NLO) calculation [11] indicates that HBChPT essentially reproduces  $d\Gamma_{\text{RMC}}/dE_\gamma$  given in Ref. [10]. A next-to-next-to-leading order (NNLO) calculation [12] has confirmed that the HBChPT expansion converges rapidly and that loop corrections to  $d\Gamma_{\text{RMC}}/dE_\gamma$  are tiny. Furthermore, a recent calculation [5] that incorporates the explicit  $\Delta$  degrees of freedom into a tree-diagram HBChPT calculation suggests that the inclusion of the  $\Delta$  modifies the spectrum only by 5%, a result consistent with the earlier finding of Beder and Fearing [13]. This change is not large enough to remove the above-mentioned anomalous  $g_P$  value. Thus the systematic analyses based on HBChPT strongly indicate that no drastic

\*Electronic address: sando@nuc003.psc.sc.edu

<sup>†</sup>Electronic address: myhrer@sc.edu

<sup>‡</sup>Electronic address: kubodera@sc.edu

<sup>1</sup>In this article OMC and RMC always refer to capture in a hydrogen target.

changes in the atomic RMC amplitudes from the existing estimates should be expected. It then seems likely that the  $d\Gamma_{\text{RMC}}/dE_\gamma$  problem is caused by the currently adopted atom-liquid translation formulas.

Meanwhile, an experiment that uses a hydrogen *gas* target to directly measure  $\Gamma_0$  with 1% accuracy is planned at PSI [14]. The use of the gas target eliminates ambiguities due to the molecular capture processes. The envisaged 1% accuracy will significantly increase precision with which the empirical value of  $g_p$  is determined. We note, however, that, to make comparison between theory and experiment at the 1% level, the existing estimate of  $\Gamma_0$  based on an HBChPT calculation up to NLO needs to be improved. First, one must ascertain that the input physical constants such as  $f_\pi$  and  $g_A$  have sufficient precision. Second, NNLO loop corrections need to be evaluated.<sup>2</sup>

In this article we present an HBChPT calculation for OMC up to NNLO in which the influence of uncertainties in the low-energy constants is carefully examined. In addition to  $\Gamma_0$  and  $\Gamma_1$ , we calculate the neutron helicity asymmetry (to be defined later). It is found that  $\Gamma_0$  obtained here is significantly larger than the previous estimates [1,4], whereas  $\Gamma_1$  essentially agrees with the literature values. The larger value of  $\Gamma_0$  is primarily due to the updated larger value of  $g_A$ . A second main point of our paper is to discuss the observational ramifications of our new estimates. If we use the new values of  $\Gamma_0$  and  $\Gamma_1$  together with the ‘‘standard’’ atom-liquid translation formulas [3], the resulting  $\Gamma_{\text{liq}}^{\text{th}}$  turns out to be significantly larger than  $\Gamma_{\text{liq}}^{\text{exp}}$  in Eq. (3), another possible indication that the existing atom-liquid translation formulas may require reexamination. We shall argue that this difficulty is probably related to the above-mentioned ‘‘anomaly’’ in RMC, and that there is possibility to resolve these two problems simply and simultaneously by invoking a molecular mixing parameter discussed by Weinberg [15].

## II. HEAVY-BARYON CHIRAL PERTURBATION THEORY (HBChPT)

HBChPT is a low energy effective field theory of QCD, which has a systematic perturbative expansion in powers of  $Q/\Lambda_\chi$ , where  $Q$  is a small typical four-momentum scale characterizing a process in question, or the pion mass  $m_\pi$ ;  $\Lambda_\chi$  is the chiral scale,  $\Lambda_\chi \approx 4\pi f_\pi \sim m_N \approx 1$  GeV. A typical scale  $Q$  in muon capture (both OMC and RMC) is the muon mass  $m_\mu = 105.7$  MeV, and hence  $Q/\Lambda_\chi \sim 0.1$ . One therefore expects a rapid convergence of relevant chiral perturbation series for muon capture; the explicit HBChPT calculations [7,12,16–18] are consistent with this expectation.

The effective chiral Lagrangian is expanded as

$$\mathcal{L} = \sum \mathcal{L}_{\bar{\nu}} = \mathcal{L}_0 + \mathcal{L}_1 + \mathcal{L}_2 + \dots \quad (4)$$

<sup>2</sup>The transition amplitude of OMC was calculated in HBChPT up to NNLO by Fearing *et al.* [17], but the capture rate was not explicitly given in that work.

The subscript  $\bar{\nu}$  denotes the order of terms,  $\bar{\nu} = d + n/2 - 2$ , where  $n$  is the number of nucleon lines and  $d$  the number of derivatives or powers of  $m_\pi$  involved in a vertex. The terms relevant to our calculation are

$$\mathcal{L}_0 = \bar{N}[iv \cdot D + 2ig_A S \cdot \Delta]N + f_\pi^2 \text{Tr} \left( -\Delta \cdot \Delta + \frac{\chi_+}{4} \right), \quad (5)$$

$$\mathcal{L}_1 = \frac{1}{2m_N} \bar{N}[(v \cdot D)^2 - D^2 + 2g_A \{v \cdot \Delta, S \cdot D\} - i(1 + b_5)[S^\alpha, S^\beta]f_{\alpha\beta}^+]N, \quad (6)$$

$$\mathcal{L}_2 = \frac{1}{(4\pi f_\pi)^2} \bar{N}[c_3 v^\alpha [D^\beta, f_{\alpha\beta}^+] + c_{13} g_A S^\alpha [D^\beta, f_{\alpha\beta}^-] + ic_{14} g_A S^\alpha [D_\alpha, \chi_-]]N + \mathcal{L}_{1/m_N^2}, \quad (7)$$

where  $\mathcal{L}_{1/m_N^2}$  is the  $1/m_N^2$  Lagrangian given in Ref. [12]. Furthermore

$$D_\mu = \partial_\mu + \Gamma_\mu, \quad (8)$$

$$\Gamma_\mu = \frac{1}{2} [\xi^\dagger, \partial_\mu \xi] - \frac{i}{2} \xi^\dagger F_\mu^R \xi - \frac{i}{2} \xi F_\mu^L \xi^\dagger,$$

$$F_\mu^{R,L} = \frac{\vec{\tau}}{2} \cdot (\vec{v}_\mu \pm \vec{a}_\mu), \quad (9)$$

$$\Delta_\mu = \frac{1}{2} \{ \xi^\dagger, \partial_\mu \xi \} - \frac{i}{2} \xi^\dagger F_\mu^R \xi + \frac{i}{2} \xi F_\mu^L \xi^\dagger, \quad (10)$$

$$f_{\mu\nu}^\pm = \frac{1}{2} (\xi^\dagger F_{\mu\nu}^R \xi \pm \xi F_{\mu\nu}^L \xi^\dagger),$$

$$F_{\mu\nu}^{R,L} = \partial_\mu F_\nu^{R,L} - \partial_\nu F_\mu^{R,L} - i[F_\mu^{R,L}, F_\nu^{R,L}], \quad (11)$$

$$\chi^\pm = \xi^\dagger \chi \xi^\dagger \pm \xi \chi^\dagger \xi, \quad \chi = m_\pi^2, \quad \xi = \exp(i\vec{\tau} \cdot \vec{\pi}/2f_\pi). \quad (12)$$

In these expressions  $\vec{v}_\mu$  and  $\vec{a}_\mu$  are the isovector vector and axial-vector external fields, respectively;  $v^\mu = (1, \vec{0})$  is the velocity four vector, and  $S^\mu = (0, \vec{\sigma}/2)$  is the nucleon spin operator. We ignore the isospin breaking effect and use  $m_N = (m_p + m_n)/2$  as the nucleon mass.<sup>3</sup> Our effective Lagrangian contains the *low energy constants* (LEC's),  $b_5$ ,  $c_3$ ,  $c_{13}$ , and  $c_{14}$ .<sup>4</sup> The LEC's,  $b_5$ ,  $c_{13}$ , and  $c_{14}$ , are finite constants

<sup>3</sup>In calculating the transition amplitudes we ignore isospin breaking but, in evaluating the phase space, we do retain the neutron-proton mass difference (see later).

<sup>4</sup>Our notations for the LEC's are different from those in Ref. [16]. The relations between them are

$$b_5 = c_6, \quad c_3 = B_{10}, \quad c_{13} = 2(4\pi f_\pi)^2 B_{24}/g_A, \quad c_{14} = B_{23}.$$

fixed by experiments. To one-loop order,  $b_5 = \kappa_V + g_A^2 m_\pi m_N / 4\pi f_\pi^2$ , where  $\kappa_V = 3.706$  is the isovector anomalous magnetic moment. The constant  $c_{13}$  is fixed by the mean square axial radius deduced from (anti) neutrino-proton scattering,  $\langle r_A \rangle = 0.65$  fm [19]; its numerical value is  $c_{13} = (4\pi f_\pi)^2 (\langle r_A \rangle^2 / 3) = 4.88$ . The parameter  $c_{14}$  is fixed by the Goldberger-Treiman (GT) discrepancy defined by

$$\Delta_{GT} \equiv 1 - \frac{g_A m_N}{f_\pi g_{\pi N}} = -\frac{2m_\pi^2}{(4\pi f_\pi)^2} c_{14}, \quad (13)$$

where  $g_{\pi N}$  is the  $\pi NN$  coupling constant. The one-loop diagrams are renormalized by  $c_3$ . Integrating in  $d = 4 - 2\epsilon$  dimension, we have

$$c_3 = -\frac{1}{6}(1 + 5g_A^2)R + c_3^R, \quad \text{with } R = \frac{1}{\epsilon} + 1 - \gamma + \ln \frac{4\pi\mu^2}{m_\pi^2}, \quad (14)$$

where  $\gamma = 0.5772 \dots$ , and the mass scale  $\mu$  is a parameter in dimensional regularization. Note that we include  $\mu$  into  $c_3^R$  to avoid the  $\mu$  dependence in the amplitudes. The parameter  $c_3^R$  is fixed by the empirical radius of the isovector Dirac form factor  $\langle r_1^V \rangle^2 = 0.585$  fm<sup>2</sup> [20]. Thus, from  $\langle r_1^V \rangle^2 / 6 = c_3^R / [(4\pi f_\pi)^2] - (1 + 7g_A^2) / 96\pi^2 f_\pi^2$ , we deduce  $c_3^R = 5.39$  (5.42) with  $g_A = 1.26$  (1.267).

### III. ATOMIC OMC RATES AND NEUTRON HELICITY ASYMMETRY: FORMALISM

The OMC process is effectively described by the current-current interaction. Thus the transition amplitude reads

$$M_{fi} = \frac{G_\mu V_{ud}}{\sqrt{2}} L_\alpha J^\alpha, \quad (15)$$

where  $G_\mu V_{ud} \equiv G_\beta$  is the Fermi constant,  $L_\alpha$  is the leptonic weak current, and  $J^\alpha$  is the nucleon weak current. The leptonic current is simply given by  $L_\alpha = \bar{u}_\nu \gamma_\alpha (1 - \gamma_5) u_\mu$ , whereas  $J^\alpha$  is a much more complex object reflecting hadron dynamics. Here we evaluate  $J^\alpha$  in HBChPT up to NNLO (one-loop) chiral order.

Since in HBChPT the nucleon current  $J^\alpha$  is expanded in terms of  $1/m_N$ , it is convenient to write  $J^\alpha$  in the Pauli-spinor form. The time and spatial components of the nucleon current  $J^\alpha = J_V^\alpha - J_A^\alpha$  are written as

$$J_V^0(q) = f_1^V(q), \quad \vec{J}_V(q) = i\vec{\sigma} \times \hat{q} f_2^V(q) + \hat{q} f_3^V(q), \quad (16)$$

$$J_A^0(q) = \vec{\sigma} \cdot \hat{q} f_3^A(q), \quad \vec{J}_A(q) = \vec{\sigma} f_1^A(q) + \hat{q} (\vec{\sigma} \cdot \hat{q}) f_2^A(q), \quad (17)$$

where we have suppressed the initial- and final-nucleon spinors as well as the common factor  $2m_N$ . The form factors,  $f_i^V$  and  $f_i^A$  ( $i = 1, 2, 3$ ), introduced here may be referred to as the nonrelativistic (NR) form factors. The relations between the NR form factors and the *standard* relativistic

nucleon weak form factors are given in the Appendix. Note that  $f_1^V$  and  $f_3^V$  are in fact related by current conservation.

The NR form factors calculated up to one-loop order in HBChPT read

$$f_1^V = 1 + \frac{c_3^R}{(4\pi f_\pi)^2} q^2 - \frac{1 + 17g_A^2}{18(4\pi f_\pi)^2} q^2 + \frac{1}{4m_N^2} \left( -\frac{3}{2} + \kappa_V \right) q^2 + \frac{1}{(4\pi f_\pi)^2} \left[ \frac{2}{3} (1 + 2g_A^2) m_\pi^2 - \frac{1 + 5g_A^2}{6} q^2 \right] f_0(q), \quad (18)$$

$$f_2^V = \left[ \frac{1}{2m_N} (1 + \kappa_V) + \frac{g_A^2}{64\pi f_\pi^2 m_\pi} q^2 + \left( \frac{g_A}{4\pi f_\pi} \right)^2 \frac{\pi(4m_\pi^2 - q^2)}{4m_\pi} m_0(q) \right] |\vec{q}|, \quad (19)$$

$$f_3^V = \frac{|\vec{q}|}{2m_N}, \quad (20)$$

$$f_1^A = g_A \left[ 1 + \left( \frac{c_{13}}{2(4\pi f_\pi)^2} - \frac{1}{8m_N^2} \right) q^2 \right], \quad (21)$$

$$f_2^A = g_A \left[ \frac{c_{13}}{2(4\pi f_\pi)^2} + \Delta_\pi(q) \left( 1 - \frac{2m_\pi^2 c_{14}}{(4\pi f_\pi)^2} + \frac{q^2}{8m_N^2} \right) \right] |\vec{q}|^2, \quad (22)$$

$$f_3^A = \frac{g_A}{2m_N} (1 - \Delta_\pi(q) q^2) |\vec{q}|, \quad (23)$$

where  $\Delta_\pi(q)^{-1} = (q^2 - m_\pi^2)^{-1}$  is the renormalized pion propagator, and the one-loop functions are given by

$$f_0(q) = \int_0^1 dx \ln [1 - x(1-x)q^2/m_\pi^2], \quad (24)$$

$$m_0(\vec{q}) = 1 - \int_0^1 dx \frac{1}{\sqrt{1 + x(1-x)\vec{q}^2/m_\pi^2}}. \quad (25)$$

The total OMC rate from a muonic hydrogen atom in a hyperfine state  $S$  is given as

TABLE I. Numerical values of the OMC form factors in Eqs. (16) and (17), calculated for each chiral order with the use of  $g_A = 1.267$  and  $g_{\pi N} = 13.4$ .

	$f_1^V$	$f_2^V$	$f_3^V$	$f_1^A$	$f_2^A$	$f_3^A$
LO	1.000	0	0	1.267	-0.426	0
NLO	0	0.248	0.053	0	0	0.045
NNLO	-0.030	-0.004	0	-0.021	0.006	0
Total	0.970	0.244	0.053	1.246	-0.419	0.045

TABLE II. Comparison of calculated atomic OMC rates.  $\Gamma_0$  ( $\Gamma_1$ ) is the capture rate [in  $s^{-1}$ ] for the initial singlet (triplet) hyperfine state. The entries for the columns labeled ‘‘This work (NNLO)’’ and ‘‘This work (NLO)’’ have been obtained with the use of  $g_A = 1.267$  and  $g_{\pi N} = 13.4$ .

	This work (NNLO)	This work (NLO)	Bernard <i>et al.</i> [26] (NNLO)	Bernard <i>et al.</i> [5] (NLO)	Primakoff [1]	Opat [4]
$\Gamma_0$	695	722	687.4	711	$664 \pm 20$	634
$\Gamma_1$	11.9	12.2	12.9	14.0	$11.9 \pm 0.7$	13.3

$$\Gamma_S = K \cdot \frac{1}{2S+1} \sum_{S_z, h} |M(h; S, S_z)|^2, \quad (26)$$

with

$$K \equiv \frac{|\phi_\mu(0)|^2}{16\pi m_\mu m_p} \left( \frac{E_\nu}{E_\nu + \sqrt{m_n^2 + E_\nu^2}} \right). \quad (27)$$

The helicity amplitude  $M(h; S, S_z)$  in Eq. (26) is specified by the final neutron helicity  $h$  ( $h=L, R$ ), the initial hyperfine spin  $S$ , and its  $z$  component,  $S_z$ . In Eq. (27),  $E_\nu$  is the final neutrino energy given by<sup>5</sup>

$$E_\nu = \frac{(m_\mu + m_p)^2 - m_n^2}{2(m_\mu + m_p)} = 99.15 \quad [\text{MeV}]. \quad (28)$$

The factor  $\phi_\mu(0)$  appearing in  $K$  is the value at the origin of the radial wave function for the  $\mu^-p$  ground state; thus  $|\phi_\mu(0)|^2 = (\alpha m_\mu^r)^3 / \pi$ , where  $\alpha$  is the fine structure constant and  $m_\mu^r = m_\mu m_p / (m_\mu + m_p)$ .

When the neutron helicity is monitored, we define the neutron helicity asymmetry as

$$\alpha_S = \frac{\Gamma_S(L) - \Gamma_S(R)}{\Gamma_S(L) + \Gamma_S(R)}, \quad (29)$$

where  $\Gamma_S(L)$  [ $\Gamma_S(R)$ ] is the rate of OMC from an initial atomic spin state,  $S$ , leading to a final left-handed (right-handed) neutron.<sup>6</sup>

In calculating the capture rates for different neutron helicities, it is convenient to choose the direction of the emitted neutrino as the  $z$  axis. In general there are eight helicity amplitudes, but with this particular choice we have only three nonzero amplitudes. They are

$$M(L; 0, 0) = \frac{\beta}{\sqrt{2}} (f_1^V + 2f_2^V + f_3^V + 3f_1^A + f_2^A + f_3^A), \quad (30)$$

$$M(L; 1, 0) = \frac{\beta}{\sqrt{2}} (f_1^V - 2f_2^V + f_3^V - f_1^A + f_2^A + f_3^A), \quad (31)$$

$$M(R; 1, -1) = \beta (f_1^V + f_3^V - f_1^A - f_2^A - f_3^A), \quad (32)$$

where  $\beta \equiv 4G_\beta m_N \sqrt{m_\mu E_\nu}$ . Correspondingly, we have  $\Gamma_0(L) = K |M(L; 0, 0)|^2$ ,  $\Gamma_0(R) = 0$ ,  $\Gamma_1(L) = K \frac{1}{3} |M(L; 1, 0)|^2$ , and  $\Gamma_1(R) = K \frac{1}{3} |M(R; 1, -1)|^2$ .

#### IV. ATOMIC OMC RATES AND NEUTRON HELICITY ASYMMETRY: NUMERICAL RESULTS

As emphasized above, at the level of precision of our concern, we need to be particularly careful about the accuracy of the input physical parameters. The most updated value of  $G_\beta$  is  $G_\beta / \sqrt{2} = 0.8030 \pm 0.0008 \times 10^{-5} \text{ GeV}^{-2}$ . For  $g_A$  and  $g_{\pi N}$ , we use as the standard values  $g_A = 1.267$  [21] and  $g_{\pi N} = 13.4$ .

Since the momentum transfer for OMC is fixed, we calculate the NR form factors for  $|\vec{q}| = E_\nu$  and  $q^2 = m_\mu^2 - 2m_\mu E_\nu$ . The results for each order of HBChPT expansion are given in Table I. The table clearly shows that the chiral perturbation series converges very rapidly. As for the helicity-dependent amplitudes, we obtain

$$\begin{aligned} M(L; 0, 0) &= 3.45 \beta, & M(L; 1, 0) &= -0.77 \beta, \\ M(R; 1, -1) &= 0.15 \beta. \end{aligned} \quad (33)$$

In Table II we give our numerical results for the atomic capture rates,  $\Gamma_0$  and  $\Gamma_1$ , along with HBChPT calculations of Bernard *et al.* [5,26]. The second column labeled ‘‘This work’’ represents the results obtained in our NNLO calculation. Comparing this column with the third column that gives the results of our NLO calculation, we note that the NNLO corrections decrease  $\Gamma_0$  significantly (3.9%). Thus it is clear that, in order to achieve theoretical precision that matches the 1% accuracy of the planned PSI experiment on  $\Gamma_0$  [14], one must take into account the NNLO terms.

We now turn to comparison with the other calculations quoted in Table II. The estimates of Primakoff [1] and Opat [4] are based on the phenomenological parametrization of the weak nucleon current with  $g_p$  fixed at its PCAC value; Primakoff retained the relativistic kinematics, whereas Opat used a nonrelativistic expansion of the amplitudes in terms of  $1/m_N$ . Bernard *et al.*'s results come from an NLO calculation [5] and an NNLO calculation [26]. The results of the two NNLO calculations, the second and fourth columns in Table II, exhibit a 1% difference. Bernard *et al.* used a different value of  $g_A$  ( $g_A = 1.26$ ). They also expanded the phase space and atomic wave function in Eq. (27) in powers of  $m_\mu/m_N$ . For the sake of comparison, suppose that, in our NNLO calculation we apply expansion of  $m_\mu/m_N$  to the

<sup>5</sup>See footnote 3.

<sup>6</sup>Thus, if the neutron helicity is not monitored,  $\Gamma_S = \Gamma_S(L) + \Gamma_S(R)$ .



TABLE III. The LEC  $c_{14}$ , atomic capture rates  $\Gamma_0$  and  $\Gamma_1$  [ $s^{-1}$ ], and the neutron helicity asymmetry  $\alpha_1$ , calculated in HBChPT up to NNLO for various choices of  $g_A$  and  $g_{\pi N}$ .

$g_A$	$g_{\pi N}$	$c_{14}$	$\Gamma_0$	$\Gamma_1$	$\alpha_1$
1.22	13.40	-2.59	656	11.3	0.865
1.24	13.40	-2.07	672	11.6	0.893
1.26	13.40	-1.54	689	11.9	0.918
1.26	13.05	-0.65	692	11.6	0.927
1.267	13.40	-1.36	695	11.9	0.925
1.267	13.05	-0.47	698	11.7	0.934

phase space, while keeping the exact atomic wave function, but ignoring neutron-proton ( $n$ - $p$ ) mass difference. Then  $\Gamma_0$  calculated up to  $1/m_N^2$  would become  $\Gamma_0^{1/m_N^2} = 708 s^{-1}$ , which is to be compared with  $\Gamma_0 = 695 s^{-1}$  in Table II. If we expand both phase space and wave function, ignoring  $n$ - $p$  mass difference, we obtain  $\Gamma_0^{1/m_N^2} = 705 s^{-1}$ . The different  $1/m_N$  expansion schemes show only a tiny numerical difference, but, the rates in both cases are enhanced by  $\sim 2\%$  compared with the exact phase space case. This is due to ignoring the nucleon mass difference; the rate is proportional to  $E_\nu^2$  and  $E_\nu$  increases by 1% when the  $n$ - $p$  mass difference is ignored. In the present work we retain the exact final phase space and atomic wave function;<sup>7</sup> viz., we apply HBChPT expansion only to the transition amplitudes. On the other hand, the 1% difference between the two NNLO calculations in Table II may stem from differences in input parameters as well.

According to Table II,  $\Gamma_0$ 's calculated in HBChPT (our present result and those of Bernard *et al.*) have significantly larger values than the earlier theoretical estimates. This is primarily due to the fact that the modern HBChPT calculations employ an updated value of  $g_A$ , which is larger than the older values. Primakoff [1] used  $g_A = 1.24$ , while Opat [4] used  $g_A = 1.22$ . In order to illustrate the sensitivity of our results to the input physical parameters, we show in Table III the values of  $\Gamma_0$  and  $\Gamma_1$  corresponding to different values of  $g_A$  and  $g_{\pi N}$ ; the LEC  $c_{14}$ , which is determined by  $g_A$  and  $g_{\pi N}$  via Eq. (13), is also listed. As can be seen from the last four rows in the table, for a given value of  $g_A$ , variations in  $g_{\pi N}$  causes only minor changes in the capture rates; even though these variations lead to a difference of a factor of  $\sim 3$  in  $c_{14}$ , the corresponding changes in the rates in the last four rows are modest; 1.3% for  $\Gamma_0$  and 2.5% for  $\Gamma_1$ . Thus the most crucial input parameter here is  $g_A$ .

Finally we discuss the helicity asymmetry. Due to the  $V-A$  weak interaction the final neutron is purely left handed when an initial atomic state is in the hyperfine singlet state ( $S=0$ ); thus we have  $\alpha_0 = 1$  as a trivial identity. For the initial hyperfine triplet state ( $S=1$ ), the final neutron can

have both left- and right-handed helicity components, and therefore  $\alpha_1$  can have a nontrivial value; our calculation gives  $\alpha_1 = 0.925$ . Thus almost all outgoing neutrons are polarized left handedly, a result consistent with Weinberg's observation [15].

## V. OMC RATES FOR LIQUID HYDROGEN TARGETS

As mentioned, in order to relate theoretical estimates of the atomic OMC rates to the capture rate measured in liquid hydrogen, one needs (in our terminology) the "atom-liquid" translation formulas. We briefly describe here the atomic and molecular physics input that underlies these formulas. A muon stopped in liquid hydrogen quickly forms a muonic atom ( $\mu$ - $p$ ) in its Bohr orbit. The atomic hyperfine triplet state ( $S=1$ ) is rapidly transformed into the singlet state ( $S=0$ ); this hyperfine transition rate is known to be  $\lambda_{10} \approx 1.7 \times 10^{10} s^{-1}$  [3], indeed a very large value. A muonic atom and a hydrogen molecule collide with each other to form a  $p$ - $\mu$ - $p$  molecule, predominantly in its ortho state (with the two proton spins parallel to each other). Let  $\lambda_{pp\mu}$  be the rate of transition from the atomic hyperfine singlet state to the ortho  $p$ - $\mu$ - $p$  molecular state. Meanwhile, the ortho  $p$ - $\mu$ - $p$  molecular state decays to the lower-lying para  $p$ - $\mu$ - $p$  molecular state. Let  $\lambda_{op}$  stand for this decay rate. Taking into account these atomic and molecular processes, one relates  $\Gamma_{\text{liq}}$ , the OMC capture rate in liquid hydrogen, to the atomic capture rates ( $\Gamma_0$  and  $\Gamma_1$ ) via the formula [3]

$$\Gamma_{\text{liq}} = \frac{\lambda_0}{\lambda_0 + \lambda_{pp\mu}} \Gamma_0 + \frac{\lambda_{pp\mu}}{\lambda_0 + \lambda_{pp\mu}} \frac{\lambda_0}{\lambda_0 + \lambda_{op}} \left( \Gamma_{om} + \Gamma_{pm} \frac{\lambda_{op}}{\lambda_0} \right), \quad (34)$$

where  $\lambda_0$  is the muon decay rate,  $\lambda_0 = 0.455 \times 10^6 s^{-1}$ . In this equation  $\Gamma_{om}$  ( $\Gamma_{pm}$ ) represents the rate of muon capture from the ortho (para)  $p$ - $\mu$ - $p$  molecular state. These rates are usually calculated using the formula

$$\Gamma_{om} = 2\gamma_O \left( \frac{3}{4} \Gamma_0 + \frac{1}{4} \Gamma_1 \right), \quad \Gamma_{pm} = 2\gamma_P \left( \frac{1}{4} \Gamma_0 + \frac{3}{4} \Gamma_1 \right). \quad (35)$$

The factors  $2\gamma_O$  and  $2\gamma_P$  account for modifications of the muon wave function as it changes from the atomic Bohr orbit to the  $p$ - $\mu$ - $p$  molecular state; according to Ref. [3],  $2\gamma_O = 1.009$  and  $2\gamma_P = 1.143$ . The validity of Eq. (35) will be discussed later in the text.

As for  $\lambda_{pp\mu}$ , there are several conflicting experimental results, see, e.g., Ref. [14]. We quote here the lowest and highest reported values:  $\lambda_{pp\mu}^{\text{exp}} = 1.89 \pm 0.20 \times 10^6 s^{-1}$ , and  $\lambda_{pp\mu}^{\text{exp}} = 2.75 \pm 0.25 \times 10^6 s^{-1}$ . The current theoretical estimate  $\lambda_{pp\mu}^{\text{th}} = 1.8 \times 10^6 s^{-1}$  lies near the lower edge of the lowest experimental value, which is a rather uncomfortable situation. Furthermore, the current experimental and theoretical values for  $\lambda_{op}$  do not agree with each other:  $\lambda_{op}^{\text{exp}} = 4.1 \pm 1.4 \times 10^4 s^{-1}$  [23] and  $\lambda_{op}^{\text{th}} = 7.1 \pm 1.2 \times 10^4 s^{-1}$  [3]. Thus it seems fair to say that the existing "atom-liquid" formulas

<sup>7</sup>We do not, however, include the finite-nucleon-size effect on the atomic wave function; this effect is known to reduce the capture rate by  $\sim 0.4\%$ , see, e.g., Appendix 1 in Ref. [22].

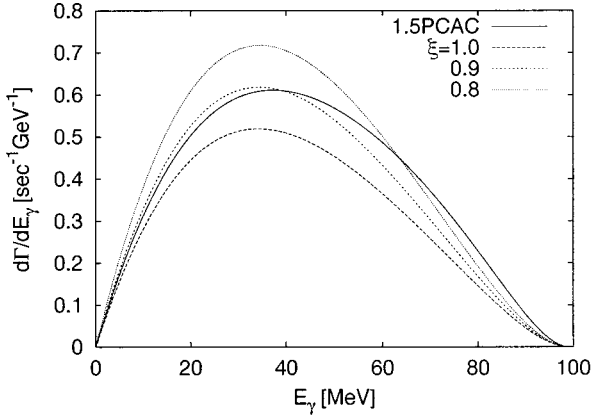


FIG. 1. The RMC photon spectrum,  $d\Gamma_{\text{RMC}}/dE_\gamma$ . The solid line labeled “1.5PCAC” is the result one would obtain from Fearing’s model if the value of  $g_p$  is assumed to be 1.5 times the standard PCAC value. The other curves represent the results of NNLO-HBChPT calculations with  $\xi=1.0, 0.9, \text{ and } 0.8$ .

are not totally free from uncertainties and that these ambiguities can affect our interpretation of the OMC rate in liquid hydrogen.

In the following we use for  $\lambda_{pp\mu}$  the value adopted in Ref. [3],  $\lambda_{pp\mu}=2.5\times 10^6 \text{ s}^{-1}$ ; for  $\lambda_{op}$ , we use two representative values:  $\lambda_{op}^{\text{th}}$  and  $\lambda_{op}^{\text{exp}}$ . Using the OMC rates of Primakoff in Table II and  $\lambda_{op}^{\text{th}}$ , Bakalov *et al.* [3] obtained  $\Gamma_{\text{liq}}=490\pm 10 \text{ s}^{-1}$ , in good agreement with the data,  $\Gamma_{\text{liq}}^{\text{exp}}=460\pm 20 \text{ s}^{-1}$ . However, if we use the values of  $\Gamma_0$  and  $\Gamma_1$  obtained in our NNLO-HBChPT calculation together with  $\lambda_{op}^{\text{th}}$ , then Eq. (34) gives a much larger rate,  $\Gamma_{\text{liq}}=518 \text{ s}^{-1}$ . If we adopt  $\lambda_{op}=\lambda_{op}^{\text{exp}}$ ,  $\Gamma_{\text{liq}}$  becomes even larger:  $\Gamma_{\text{liq}}=532 \text{ s}^{-1}$ . Thus the use of the updated values of  $\Gamma_0$  and  $\Gamma_1$  as obtained here in combination with the commonly used “atom-liquid translation formulas” spoils the previously reported *good* agreement between  $\Gamma_{\text{liq}}^{\text{th}}$  and  $\Gamma_{\text{liq}}^{\text{exp}}$ . So, in addition to the problem of the RMC photon spectrum discussed in the Introduction, another serious problem seems to be lurking in the OMC sector.

## VI. A MIXING MOLECULAR PARAMETER TO FIT THE OMC AND RMC DATA

In view of the fact that these two problems occur in the experiments involving liquid hydrogen targets, it seems of interest and of importance to reexamine the reliability of the formulas hitherto used in the literature to relate the atomic capture rates to  $\Gamma_{\text{liq}}$ . Although a thorough investigation of this issue is beyond the scope of this article, we wish to discuss here a particular aspect of molecular physics input which seems relevant to the present issue but so far has not been fully examined. Taking up an early observation made by Weinberg [15], consider the possibility that in liquid hydrogen two ortho molecular  $p\text{-}\mu\text{-}p$  spin states,  $S_{p\mu p}=1/2$  and  $3/2$  may be populated. If this indeed happens,  $\Gamma_{om}$  in Eq. (35) should be replaced with

$$\Gamma'_{om}=\xi\Gamma_{om}(1/2)+(1-\xi)\Gamma_{om}(3/2), \quad (36)$$

TABLE IV. The OMC rate in liquid hydrogen,  $\Gamma_{\text{liq}} [\text{s}^{-1}]$ , calculated for five different values of the molecular mixing parameter  $\xi$ , Eq. (36), and for two typical choices (explained in the text) of  $\lambda_{op}$ , the ortho-to-para transition rate in a  $p\text{-}\mu\text{-}p$  molecule. The second (third) row corresponds to the use of  $\lambda_{op}^{\text{th}}=7.1\times 10^4 \text{ s}^{-1}$  ( $\lambda_{op}^{\text{exp}}=4.1\times 10^4 \text{ s}^{-1}$ ).

$\xi$	1.0	0.95	0.90	0.85	0.80
$\Gamma_{\text{liq}}(\lambda_{op}^{\text{th}})$	518	499	480	461	442
$\Gamma_{\text{liq}}(\lambda_{op}^{\text{exp}})$	532	512	492	472	452

where  $\Gamma_{om}(1/2)=\Gamma_{om}$  of Eq. (35) and  $\Gamma_{om}(3/2)=2\gamma_O\Gamma_1$ . According to Weinberg [15], the mixing parameter  $\xi$  can be in the range of  $0.5\leq\xi\leq 1$ . Only theoretical estimates of  $\xi$  exist, and its literature value is  $\xi\approx 1$  [24,3]; to our knowledge  $\xi$  has never been measured experimentally. To study the consequences of  $\xi\neq 1$ , we have calculated  $\Gamma_{\text{liq}}$  with the use of Eqs. (34)–(36), for several values of  $\xi$ . For  $\Gamma_0$  and  $\Gamma_1$  we have used the results of our NNLO calculation while for  $\lambda_{op}$  we have considered the two representative values discussed above:  $\lambda_{op}^{\text{th}}$  and  $\lambda_{op}^{\text{exp}}$ . The results are shown in Table IV. The table indicates that, if  $0.8\leq\xi\leq 0.9$ , the theoretical and experimental values of  $\Gamma_{\text{liq}}$  are in good agreement.<sup>8</sup>

We next argue that the introduction of  $\xi$  in this range leads to resolution of the RMC problem as well. We first remark that Eqs. (34)–(36), can be used, *mutatis mutandis*, for RMC as well, in particular, for calculation of  $d\Gamma_{\text{RMC}}/dE_\gamma$ , the photon spectrum for RMC in liquid hydrogen. With the atomic RMC transition amplitudes previously obtained in a NNLO-HBChPT calculation [12], we have evaluated  $d\Gamma_{\text{RMC}}/dE_\gamma$  for various values of  $\xi$ ; the other atomic and molecular population parameters are kept fixed at the values used in Ref. [9]: 6.1% atomic hyperfine singlet state, 85.4% ortho  $p\text{-}\mu\text{-}p$  state and 8.5% para  $p\text{-}\mu\text{-}p$  state. The results are shown in Fig. 1. The dashed line (lowest curve) represents the no-mixing case,  $\xi=1$ , which corresponds to  $d\Gamma_{\text{RMC}}/dE_\gamma$  obtained in Ref. [12]. For comparison, we also show in the figure (the solid line) the result obtained in a modified version of the Fearing model [10] wherein  $g_p$  is taken to be 1.5 times the PCAC value. This line represents the best fit curve to the observed  $d\Gamma_{\text{RMC}}/dE_\gamma$  in the analysis reported in Refs. [8,9]. One can see from the figure that  $\xi$  in the range of 0.8–0.9 leads to a photon spectrum that is satisfactorily close to the “observed” spectrum (solid line) for  $E_\gamma\geq 60 \text{ MeV}$ .

## VII. DISCUSSION AND CONCLUSIONS

We have considered in our HBChPT calculation up to NNLO contributions. Some remarks on possible higher order effects are in order here. As discussed in Ref. [5], a one-loop

<sup>8</sup>If one replaces Eq. (34) with an older and simpler “atom-liquid” formula of Ref. [23], the OMC data can be fit with  $\xi=1$ , and the RMC data with  $\xi\approx 0.95$  within the framework of an NLO-HBChPT calculation, see Ref. [26].

diagram in  $N^3\text{LO}$  which contains a vertex with the anomalous magnetic moment,  $\kappa_V m_\mu/m_N \sim 0.5$ , can be comparable in size to the NNLO diagrams. This means that the correction to the capture rate due to the  $N^3\text{LO}$  terms may reach the 1–2 % level. Thus, for a more precise theoretical prediction of the OMC rates, it can in principle be important to include the  $N^3\text{LO}$  corrections, although the existing uncertainty in the values of  $g_A$  and  $g_{\pi N}$  may not warrant the effort. Moreover, at the level of  $N^3\text{LO}$ , the isospin breaking effects as well as QED corrections [25] are expected to give sizable contributions.

In conclusion, we have carried out a HBChPT calculation of the atomic OMC rates to next-to-next-to-leading order. Our result indicates that, once the measurement of the hyperfine-singlet atomic OMC rate reaches 1% accuracy, as envisaged in a PSI experiment, theoretical predictions based on HBChPT must include at least NNLO corrections. Furthermore, we have shown that both the OMC rate and the RMC photon energy spectrum measured in liquid hydrogen can be reproduced by introducing the molecular mixing parameter  $\xi$  in the range of  $\xi \sim 0.8\text{--}0.9$ . It seems interesting to examine whether this range of  $\xi$  is realistic.

Finally, we have shown that the neutron helicity asymmetry for OMC from a hyperfine triplet state is  $\sim 93\%$ .

#### ACKNOWLEDGMENTS

The authors are grateful to Véronique Bernard, Thomas Hemmert, and Ulf Meissner for kindly communicating the content of Ref. [26] and for extremely useful discussions. This work is supported in part by the NSF Grant No. PHY-9900756.

#### APPENDIX

Assuming the absence of the second-class current, one can express the nucleon vector and axial currents in terms of four form factors:

$$J_V^\alpha = \bar{u}_n(p') \left[ G_V(q) \gamma^\alpha + G_M(q) \frac{i\sigma^{\alpha\beta} q_\beta}{2m_N} \right] u_p(p), \quad (\text{A1})$$

$$J_A^\alpha = \bar{u}_n(p') \left[ G_A(q) \gamma^\alpha \gamma_5 + G_P(q) \frac{q_\beta}{m_\mu} \gamma_5 \right] u_p(p), \quad (\text{A2})$$

where  $G_V(q)$ ,  $G_M(q)$ ,  $G_A(q)$ , and  $G_P(q)$  are the vector, weak-magnetism, axial-vector, and pseudoscalar form factor, respectively;  $q = p' - p$  and  $u_p$  ( $u_n$ ) is the Dirac spinor for the proton (neutron). These standard relativistic form factors are related to the NR form factors,  $f_i^V$ 's and  $f_i^A$ 's, defined in Eq. (17). Up to  $\mathcal{O}(1/m_N^2)$

$$f_1^V = G_V(q) \left( 1 - \frac{q^2}{8m_N^2} \right) + \frac{q^2}{4m_N^2} G_M(q),$$

$$f_2^V = \frac{1}{2m_N} [G_V(q) + G_M(q)] |\vec{q}|, \quad f_3^V = \frac{1}{2m_N} G_V(q) |\vec{q}|,$$

$$f_1^A = G_A(q) \left( 1 - \frac{q^2}{8m_N^2} \right), \quad f_2^A = -\frac{G_P(q)}{2m_\mu m_N} \left( 1 + \frac{q^2}{8m_N^2} \right) |\vec{q}|^2,$$

$$f_3^A = \frac{1}{2m_N} \left( G_A(q) + \frac{G_P(q) q^2}{2m_\mu m_N} \right) |\vec{q}|.$$

- 
- [1] H. Primakoff, in *Nuclear and Particle Physics at Intermediate Energies* (Plenum, New York, 1975).
- [2] G. Bardin *et al.*, Nucl. Phys. **A352**, 365 (1981).
- [3] D. D. Bakalov, M. P. Faifman, L. I. Ponomarev, and S. I. Vinitzky, Nucl. Phys. **A384**, 302 (1982).
- [4] G. I. Opat, Phys. Rev. **134**, B428 (1964).
- [5] V. Bernard, T. R. Hemmert, and U.-G. Meissner, FZJ-IKP(TH)-2000-02, nucl-th/0001052 v.1.
- [6] V. Bernard, N. Kaiser, and U.-G. Meissner, Phys. Rev. D **50**, 6899 (1994).
- [7] V. Bernard, H. W. Fearing, T. R. Hemmert, and U.-G. Meissner, Nucl. Phys. **A635**, 121 (1998); **A642**, 563 (1998).
- [8] G. Jonkmans *et al.*, Phys. Rev. Lett. **77**, 4512 (1996).
- [9] D. H. Wright *et al.*, Phys. Rev. C **57**, 373 (1998).
- [10] H. W. Fearing, Phys. Rev. C **21**, 1951 (1980).
- [11] T. Meissner, F. Myhrer, and K. Kubodera, Phys. Lett. B **416**, 36 (1998).
- [12] S. Ando and D.-P. Min, Phys. Lett. B **417**, 177 (1998).
- [13] D. Beder and H. W. Fearing, Phys. Rev. D **35**, 2130 (1987).
- [14] D. V. Balin *et al.*, PSI proposal No. R-97-05.1, 1996.
- [15] S. Weinberg, Phys. Rev. Lett. **4**, 575 (1960).
- [16] V. Bernard, N. Kaiser, and U.-G. Meissner, Int. J. Mod. Phys. E **4**, 193 (1995).
- [17] H. W. Fearing, R. Lewis, N. Mobed, and S. Scherer, Phys. Rev. D **56**, 1783 (1997).
- [18] H. W. Fearing, R. Lewis, N. Mobed, and S. Scherer, Nucl. Phys. **A631**, 735c (1998).
- [19] T. Kitagaki *et al.*, Phys. Rev. D **28**, 436 (1983); L. A. Ahrens *et al.*, *ibid.* **35**, 785 (1987); L. A. Ahrens *et al.*, Phys. Lett. B **202**, 284 (1988).
- [20] P. Mergell, U.-G. Meissner, and D. Drechsel, Nucl. Phys. **A596**, 367 (1996).
- [21] Particle Data Group, D. E. Groom *et al.*, Eur. Phys. J. C **15**, 1 (2000).
- [22] J. Govaerts and J.-L. Lucio-Martinez, Nucl. Phys. **A678**, 110 (2000).
- [23] G. Bardin *et al.*, Phys. Lett. **104B**, 320 (1981).
- [24] A. Halpern, Phys. Rev. **135**, A34 (1964).
- [25] G. Müller and U.-G. Meissner, Nucl. Phys. **B556**, 265 (1999).
- [26] V. Bernard, talk at the Chiral Dynamics 2000 Workshop, Jefferson Laboratory, Virginia, 2000; V. Bernard, T. R. Hemmert, and U.-G. Meissner, Nucl. Phys. A (to be published).